PHYSICAL REVIEW C VOLUME 10, NUMBER 5 NOVEMBER 1974

Coupled-channel calculations of electron scattering by samarium*

R. L. Mercer
Speech Processing Group, Computer Sciences Department, International Business Machines Corporation, Thomas J. Watson Research Center, Yorktown Heights, New York 10598

D. G. Ravenhall
Physics Department, University of Illinois, Urbana, Illinois 61801
(Received 25 February 1974)

The coupled-channel method is considered in the context of relativistic hadron or lepton scattering by nonspherical dynamical nuclei. The program Zenith, which calculates electron-nucleus scattering via Coulomb and magnetic multipole potentials, is described and is applied in particular to the deformed samarium isotopes ^{152}Sm and ^{154}Sm. Two- and three-level calculations for the ground state 0+ and the excited states 2+ and 4+ containing all relevant $l=0$, 2, and 4 Coulomb potentials are described. The elastic dispersion effect, arising mainly from coupling with the 2+ first excited state, and the dispersive effect on the $0+ \rightarrow 2+$ inelastic cross section, coming mainly from the diagonal $l=2$ scattering in the excited state, are appreciable at 105 MeV, the highest energy at which measurements have been made. The largest effect, however, is that on the $0+ \rightarrow 4+$ inelastic cross section arising from the sequential excitation $0+ \rightarrow 2+ \rightarrow 4+$ via the $l=2$ potential. It has interesting small-angle behavior and becomes greater than 20% at the largest measured angles at 105 MeV. The dependence of some of these effects on energy and q_{eff} is explored up to 250 MeV and 2 fm^{-1}.

[NUCLEAR REACTIONS ^{152,4}Sm(e, e') calculations, coupled channels, 50 MeV < E < 250 MeV. Dispersive effects on elastic and inelastic cross sections.]

I. INTRODUCTION

The use of electron scattering to explore nuclear charge shapes and charge-current transition densities is simple and direct. It is customary in analyzing experimental differential cross sections to use a partial-wave analysis for the elastic cross section and a distorted-wave treatment for the inelastic cross sections. The assumption underlying such a treatment is that while the nuclear Coulomb monopole field is strong enough to distort the electron wave functions significantly, the multipole transition potentials are weak enough that they need be treated only to first order. While this is usually a very good approximation, there is a body of work exploring the extent to which the latter assumption can affect elastic and inelastic scattering.[1] With various choices concerning the important intermediate states and multipole potentials, and with various calculational techniques, the general conclusion may be summarized as that the effect on elastic scattering of second-order virtual excitation, the so-called dispersion effect, is fairly small, of order a few percent in diffraction minima and much less elsewhere. There are, however, some exceptions to this general conclusion. It has been suggested that at rather low energies, 50 to 120 MeV, dispersion effects can be quite large, of order 10 to 20% for titanium isotopes, for example.[2] These large effects are thought to be associated with the occurrence of low-lying nuclear excited states strongly coupled to the ground state. Such a source of dispersion effects is presumably a nucleus-to-nucleus variation on the universal dispersion contributions arising from transitions to intermediate states common to all nuclei, such as the giant collective states and the high-lying quasifree nucleon states.[3] The latter contributions are the subject of most of the studies summarized in Ref. 1. They must be included in any complete description of the electron-nucleus scattering process. The topic of the present paper, however, is confined to the former contributions to dispersive effects.

The general problem of electron scattering by a physical nucleus, including virtual excitation to all levels, is clearly very difficult. The much more restricted problem in which nuclear excitation is confined to a few low-lying levels is a finite problem in wave mechanics, and as such it is possible to contemplate an exact solution to it. The straightforward application of standard quantum mechanical techniques results in the coupled-chan-

nel method, various applications of which exist in the literature. The special difficulties which the electron-scattering problem presents are associated with the relativistic dynamics and with the high accuracy which current experiments demand. This accuracy requirement makes it desirable if possible to avoid approximations such as Rawitscher's assumption[4] of monopole excitation to one state only, or the use of the eikonal approximation[5] by Brown and Kujawski and Rosenfelder. What we have attempted is a direct solution of the coupled-channel problem, with no further approximation[6] than that of confining excitation to a few nuclear levels.[7] We are aware, of course, of the success of a coupled-channel calculation of energy levels of muonic atoms.[8] We comment on its relationship to our work later.

As will become evident, the computation scheme we have chosen, and the program Zenith which realizes it,[9] are quite complex. They are in fact not yet in final form, but are undergoing minor changes as we examine more complicated physical situations. As a testing ground with potentially the largest possible dispersion effects, we have considered the deformed samarium isotopes. A beautiful experiment on $^{152}_{60}$Sm has been reported by an MIT-NBS collaboration.[10] It has been analyzed by that group with a one-channel partial-wave program for the elastic scattering and with distorted-wave Born approximation for the excitation to the 2+ and 4+ excited states. Our conclusion, reported later in this paper, is that at the energies used (up to 105 MeV) the dispersive effects on the elastic and on the $0+ \rightarrow 2+$ inelastic scattering are not overwhelming, but are big enough to change appreciably the detailed results of that analysis. The sequential $0+ \rightarrow 2+ \rightarrow 4+$ contribution to the $0+ \rightarrow 4+$ excitation is quite substantial, and certainly needs inclusion. We have, as yet, examined only a few of the properties of these dispersive effects and how they depend on the problem parameters. What we present here, therefore, is a report on the magnitude and extent of the particular effects expected in ^{152}Sm, and also in ^{154}Sm, an even more deformed nucleus. We examine the dependence of the elastic dispersion effect on energy and angle, and the inadequacy of representing it as a function of the recoil momentum q alone. We do not, however, examine the dependence on the atomic number or the behavior of multipoles other than the quadrupole and hexadecapole potentials present in ^{152}Sm. We hope in future work to make detailed comparisons with previous approximate calculations on other nuclei.[1,2]

The algebra and arithmetic of the method, given in detail in Ref. 9, are too complicated to repeat in detail here. In Sec. II we give, therefore, a description of the principles of the method, making reference to and comparison with the customary single-channel partial-wave method, but without equations. The program Zenith and the tests it has undergone are described in Sec. III. Cross sections calculated with Zenith for ^{152}Sm are given in Sec. IV together with percentage dispersive effects. A more extensive examination of the variation of the dispersive effects with some charge-distribution parameters, all for ^{154}Sm, are given in Sec. V. A suggested procedure for data analysis is given in Sec. VI.

II. COUPLED-CHANNEL METHOD

Calculation of charged-particle potential scattering by the partial-wave method, encountered in hadron or lepton elastic scattering by a spin-zero nucleus, proceeds in three stages: calculation of the Coulomb monopole potential from the assumed nuclear charge distribution (assuming that the hadronic potentials are given explicitly as functions of the radius); integration of the radial wave equation corresponding to each eigenstate of the incident particle's total angular momentum $\vec{J}$ and parity P to obtain the phase shift for each j, p; and summation of the Legendre series containing the phase shifts, to obtain the elastic scattering amplitude and differential cross section. The central time-consuming task, however, is the second stage. Out to a radius $r = R_{\max}$, which encloses all of the nuclear charge (and all of the optical potentials for hadronic interactions), the potential depends on the particular nuclear radial density function being used, and the wave equation must be integrated from the origin to $R_{\max}$ step by step. The wave function achieves the simple sinusoidal form which defines the phase shift (or may be well approximated by an asymptotic series of which this is the leading term) at a radius $r = R_{\text{asym}}$ which for large j is considerably larger than $R_{\max}$. In the region $r > R_{\max}$ the only remaining potential, the Coulomb monopole potential, assumes the simple form Ze^2/r, and for this case there exist solutions—Coulomb functions—whose analytic properties are known. In particular, the Coulomb functions whose behavior at $r = 0$ is regular or irregular in a standard way, have Coulomb phase shifts at infinity for which analytic expressions are available. The phase shifts for the potential of interest may be obtained, therefore, by comparing each radial wave function with the corresponding known Coulomb functions at $r = R_{\max}$, thus avoiding further numerical integration out to R_{asym}. It is necessary to have calculated the Coulomb functions previous-

ly, of course, but this need only be done once for a particular Z and R_{max} (and the energy E, if the incident particle's mass is not neglected). In the final process, summation of the Legendre series containing the phase shifts to obtain the scattering amplitude, a procedure such as the reduction method[11] is needed to make this Coulomb series converge. To reproduce well the $1/\sin^2\frac{1}{2}\theta$ singularity of the elastic amplitude, additional terms are added to the Legendre series containing, for j-values beyond those for which the numerical integration has been performed, just the point-Coulomb phase shifts, i.e. the phase shifts of the regular Coulomb functions.

For the more complex system of a charged hadron or lepton interacting with a nucleus of spin I_0 through various allowed electromagnetic and hadronic multipole potentials, a partial wave decomposition is still possible, in terms of eigenstates of the total angular momentum $\vec{F}=\vec{I}+\vec{J}$. Instead of separate radial wave equations for each j and p there now occur sets of $2I_0+1$ coupled radial equations for each F and p. (For $F<I_0$ the number is less than $2I_0+1$.) Each radial equation is either a second-order differential equation or two coupled first-order equations, of course. The added feature of a dynamical nucleus with various states of spin I_i has the effect of increasing the number of coupled radial wave equations to $n_{eq}=\sum_i(2I_i+1)$ (for large F), but does not prevent the partial-wave decomposition.

The first stage of the calculation, the preparation of the potentials from the various charge, current, and magnetization densities, is straightforward. For the second state, each set of n_{eq} pairs of first-order ordinary differential equations for a given F has n_{eq} independent solutions which are regular at $r=0$. The complete wave function with proper asymptotic boundary conditions is an as yet unknown superposition of the n_{eq} regular solutions, so that all of them must be considered. The integration from the origin to R_{max} must be done step by step, as in potential scattering. It is now n_{eq}^2 times more time consuming, so good computational technique is at a premium, but there is no way to avoid it in an exact calculation. In the region $r>R_{max}$ the electromagnetic potentials have achieved their simple asymptotic forms $v_l(r)\sim s_l r^{-1-l}$ for multipolarity l. Except for the especially simple case of monopole excitation, where $v_0(r)$ vanishes with the nuclear density (and is thus zero at R_{max}) the other multipole potentials are not negligible compared with the Coulomb monopole potential. Thus exterior functions analogous to the Coulomb functions depend on all of the multipole potential strengths s_l, i.e., on all of the B (C, E, or $M\lambda$) for the nuclear levels and transitions involved, as well as on the nuclear charge Z and the energy E. To our knowledge there exist no analytic expressions for these generalized relativistic Coulomb functions. Clearly their dependence on all of the strengths makes impracticable the potential-scattering approach of having a library of Coulomb functions calculated previously for appropriate parameter values. The new problem encountered, comparing the coupled-channel situation to that of potential scattering, is thus to calculate the asymptotic properties for the n_{eq} coupled equations. This requires that we first find, at some $r=R_{asym}$, an asymptotic form from which it is possible to reconstruct the complete wave function, with proper boundary conditions of incoming waves in only the ground-state channels. We must then carry the n_{eq} interior solutions from R_{max} to R_{asym}.

In the program Zenith, the procedure adopted to arrive at the asymptotic forms is as follows. The possibility of an asymptotic expansion of the coupled equations is indicated by the fact that all $l\neq 0$ potentials fall off faster than the Coulomb $l=0$ potentials, so that the latter dominate the phase behavior. Starting with leading terms in the expansion in $1/r$ which resemble those of the Coulomb-function asymptotic expansion, a matrix relationship may be established between succeeding coefficients in the expansion. Thus for a given set of multipole potentials $s_l r^{-1-l}$, asymptotic expansions may be attempted, and if $r=R_{asym}$ is chosen sufficiently large, they will converge to some desired accuracy ϵ. There are in fact $2n_{eq}$ sets of asymptotic solutions, since there are n_{eq} coupled Dirac or Klein-Gordon equations, each effectively of second order. We adopt a standard definition for these solutions, and call them the "regular and irregular Coulomb functions," but the nature of their behavior at $r=0$ is not known.

The integration of the n_{eq} interior solutions from R_{max} out to the perhaps quite large R_{asym} is too time consuming for a step-by-step integration. We observe, however, that in this region the potentials all have simple power-law dependence on r. This simple behavior then makes practicable an expansion of the solutions about some point $r=r_0$ (where initially $r_0=R_{max}$) in a power series for which the coefficients may be obtained recursively in matrix form. Since the singular points of the system of equations being solved are at $r=0$ and $r=\infty$, the power series expansion about r_0 has radius of convergence equal to r_0, and so converges out to $r=2r_0$. Thus, in principle, the solutions may be continued out from $r=R_{max}$ in successively greater steps, each doubling the previous value of r. There are, however, practical limitations imposed by computer word length and

loss of accuracy when partial sums become too large compared with the final converged sum. These "giant steps" are thus of limited size. But they are many times the step-size needed in the interior integration. The magnitude of the giant steps and the number of terms in the expansion may be optimized to produce an integration scheme which is ten to a hundred times faster than step-by-step integration. Even for monopole potential scattering, it may be used as a practicable alternative to the method, mentioned earlier, of maintaining a library of Coulomb functions.

Comparison of the n_{eq} interior solutions at R_{asym} with the $2n_{eq}$ generalized Coulomb functions reveals the asymptotic character (phases and amplitudes of the various channel components) of these n_{eq} solutions. Since each is regular at the origin and now has known asymptotic form, it is a matter of $n_{eq} \times n_{eq}$ matrix algebra to determine the unique superposition which corresponds to the scattering boundary condition of incoming waves of appropriate amplitudes in only the ground-state channels. This scattering wave function has certain amounts (amplitude and phase) of outgoing waves in each channel component. After this procedure has been followed for a sufficient number of F (total angular momentum) states the Legendre series for the desired elastic and inelastic processes may be compiled from the appropriate channel components. These Legendre series have the nonconvergence properties characteristic of all Coulomb-scattering problems, of course, and we sum them by the reduction method.[11] The foregoing method does not allow us to supplement the Legendre series with the terms corresponding, in potential scattering, to the regular point-Coulomb phase shifts, since we do not possess the asymptotic expansion belonging to the generalized Coulomb functions regular at the origin. (The origin is, in general, an irregular singular point of the coupled equations with point potentials.) We have a prescription which appears to work well for the elastic amplitude, namely to add the uncoupled point-Coulomb phase shifts for higher F values. Since the inelastic Legendre series has better convergence properties than the elastic series, the problem is not so pressing for them. We are working on a method to generate these terms rapidly.

At this point comparison should be made with the corresponding solution to the bound-state problem, made by McKinley[8] several years ago. The asymptotic solutions of the bound-state problem must decay exponentially with r, so that there are only n_{eq} different sets. Their asymptotic expansions follow readily from the coupled equations, which may be integrated inwards to R_{max} in a stable manner. The successful matching of the interior and exterior sets of n_{eq} equations signals the correct choice of the energy eigenvalue. The scattering and bound-state problems thus differ mainly in their treatments of the exterior solutions. We have not in fact used the formalism or computational methods of McKinley's program, since we wished to be free of any conceptual commitments in our search for a fast code.

III. PROGRAM ZENITH

Zenith has been constructed, using the Dirac equation, to calculate scattering of a spin-$\frac{1}{2}$ particle of arbitrary charge and mass. At present it contains only Coulomb and magnetic multipole potentials. None of these particular choices is mandatory on the method, and we hope to construct versions of Zenith containing other interesting possibilities.[12] In one respect, however, the method is at present necessarily less general than our description implies: The asymptotic expansion may be summed in the general multipolarity case only if all of the channels are degenerate in energy, i.e. only if we make nuclear excitation energies equal to zero. The expansion does work, even with nondegenerate channels, if the channels are not coupled at R_{asym}. We may thus gauge the extent of the approximation made in the general case, when we perforce neglect excitation energies, by considering the effect of nondegeneracy in some equivalent monopole-excitation case, or in the artificial situation obtained by applying a "convergence factor" to the off-diagonal multipole potentials so that they become negligible at $r = R_{asym}$. This factor spoils the low-q behavior of the inelastic differential cross sections, of course. In the particular situations considered here, we believe by these comparisons that nondegeneracy is of negligible importance in the results we obtain. We hope in the future to remove this deficiency in the method.

Since in several respects the computations attempted by Zenith go beyond our previous experience, the choice of appropriate values for the many internal parameters has been a matter of experiment. As yet, few of them can be safely made automatic, especially if a new physical situation (more states, higher spins, different multipoles) is attempted. There are, furthermore, places where we are still developing the method. Thus at present we regard Zenith as still in the experimental stage. The limitation as regards magnitude of the system examined (i.e., number and spins of states) depends on the computer fast-storage available, and as regards incident energy and nuclear size it seems at present to be a

ter only of computational expense. We give further details at the end of Sec. IV.

We mention briefly the tests that Zenith has undergone which lead us to believe that its new predictions are reliable. One-state $I_0=0$ (nuclear spin) zero-mass electron scattering agrees completely with an earlier program used extensively for elastic scattering studies.[13] Finite mass one-state calculations agree to the expected extent with corresponding calculations made with the Klein-Gordon potential-scattering program of Clark.[14] One-state $I_0=\frac{1}{2}$ pure $M1$ interaction and $I_0=1$ pure $E2$ interaction, with zero Coulomb monopole contribution, agree with Born approximation.[9] It should be observed that this is a meaningful and stringent test for a partial-wave calculation, since unlike distorted-wave calculations, the Born approximation integral is in no sense built into the method, but must be arrived at by correct summation of the individual F contributions. Coulomb monopole excitation with zero excitation energy agrees with the results obtained by the difference method[4] using any of our one-state programs to generate the $v_0 \pm v_{ex}$ scattering amplitudes.

A two-state calculation, modeling for example the common situation of a 0+ ground state and a 2+ excited state coupled by a quadrupole $C2$ interaction, produces both elastic and inelastic scattering differential cross sections. The latter may be compared with inelastic experiments or with distorted-wave Born approximation (DWBA) fits to them. Both contain all of the effects of the virtual excitations associated with these levels and this coupling. We should be able to reproduce both DWBA and one-state elastic results to arbitrary accuracy by suitably reducing the $C2$ coupling strength. By also reducing the $C0$ coupling strength (i.e., Z) we may reproduce pure Born approximation. The checks we have made include comparisons with simple DWBA theory (dependence on effective q, and on $C0$ strength, etc.) and comparisons with published curves.[9] We are at present attempting detailed checks with HEINEL [15] for sample cases, but in view of the other tests that Zenith has already passed, we do not think that any major errors remain.

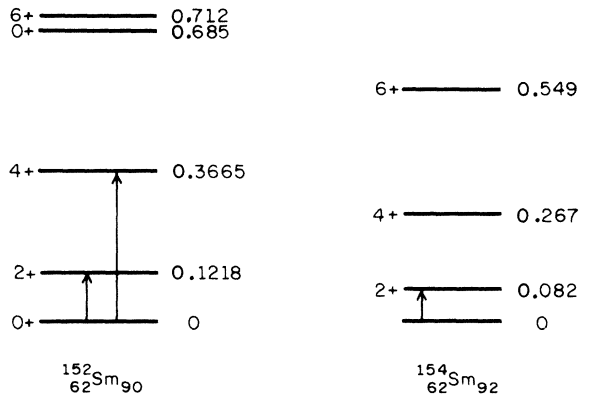

FIG. 1. Level schemes for the nuclei investigated, with energies in MeV. In ^{152}Sm, the MIT-NBS analysis (Ref. 10), whose values are used in this paper, assume $\langle r^2\rangle_{el}^{1/2}=5.0922$ fm; $B_{0+\to 2+}(E2)=3.377\times10^4\ e^2\,\mathrm{fm}^4$, $B_{0+\to 4+}(E4)=1.345\times10^7\ e^2\,\mathrm{fm}^8$. For our investigation in ^{154}Sm, we use $B_{0+\to 2+}(E2)=4.61\times10^4\ e^2\,\mathrm{fm}^4$ (Ref. 21) and the same undeformed shape as in ^{152}Sm.

IV. RESULTS FOR ^{152}Sm

The nucleus is rotational with the level scheme shown in Fig. 1. The MIT-NBS analysis[10] of electron scattering cross sections, elastic and inelastic to the 2+ and 4+ levels, at energies from 50 to 105 MeV, gives the following nuclear model parameters[16]: The intrinsic Fermi shape

$$\rho(c_0, z_0; r)=\rho_0\{\exp[(r-c_0)/z_0]+1\}^{-1} \tag{1}$$

is deformed into the shape $\rho(\vec{c}, z_0; \vec{r})$ by the radius variation[17]

$$\vec{c}=c_0\left[1+\sum_{l=2}\beta_l Y_{l0}(\theta_{cr})\right], \tag{2}$$

where $c_0=5.7573$ fm, $z_0=0.6014$ fm, $\beta_2=0.2896$, $\beta_4=0.070$, and $\beta_6=-0.012$. The multipole charge distributions $\rho_l(r)$ defined by

$$\rho(\vec{c}, z_0; \vec{r})=\sum_{l=0}\rho_l(r)Y_{l0}(\theta_{cr}), \tag{3}$$

obtained numerically, produce $l=2$ and $l=4$ transition charge distributions such that $B_{0+\to 2+}(E2)=3.377\times10^4\ e^2\,\mathrm{fm}^4$, $B_{0+\to 4+}(E4)=1.345\times10^7\ e^2\,\mathrm{fm}^8$, and an $l=0$ charge distribution with $\langle r^2\rangle^{1/2}=5.0922$ fm. We have made no fits to experimental data, but have used this completely prescribed nuclear model to calculate various effects introduced by the coupled-channel method.[18]

With such a necessarily complex nuclear model, possible parameter variations are too numerous to contemplate. We restrict our present considerations of the three-level system to two coupling

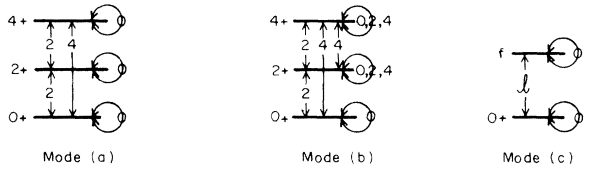

FIG. 2. Coupling modes used in coupled-channel calculations with ^{152}Sm. The lines and loops terminating in arrows indicate the various diagonal and transition potentials, with their multipolarities.

modes: (a) the scheme illustrated in Fig. 2(a), where besides the monopole potentials there are only the $l=2$ and 4 transition potentials linking the 0+, 2+, and 4+ levels; (b) the scheme with all $l=0$, 2, and 4 diagonal and transition potentials which can link the three states, as shown in Fig. 2(b). Mode (a) permits inelastic scattering and allows us, by comparison with single-state elastic scattering or with DWBA inelastic scattering, to calculate the part usually considered important among the dispersion effects due to these levels. (See, however, Ref. 3.) It also allows us to obtain the contribution to 0+ → 4+ excitation from the sequential 0+ → 2+ → 4+ transitions. From mode (b), the complete scheme for these three levels, we can check what other contributions are left out by the simpler coupling scheme. All calculations in this section have been made with the approximations that the electron mass and the nuclear excitation energies can be neglected. We examine the quite unimportant effect of these approximations in the next section.

In Fig. 3 are shown differential cross sections at an incident energy of 105 MeV, obtained with coupling mode (a). Inset in that figure are the

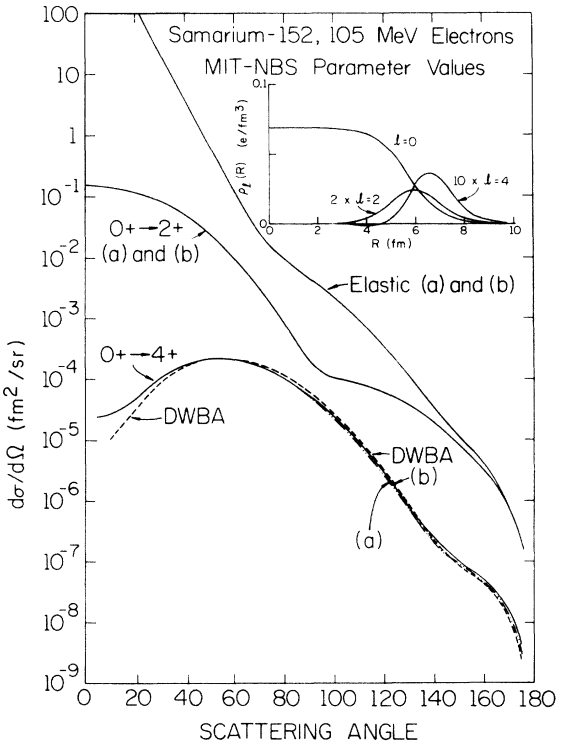

FIG. 3. Differential cross sections for 105 MeV electrons on ^{152}Sm, obtained with Zenith calculating in modes (a) and (b). The nuclear model, obtained by the MIT-NBS group (Ref. 10), is described in Sec. IV. Inset are plots of the multipole charge densities $\rho_l(r)$ defined by Eq. (3).

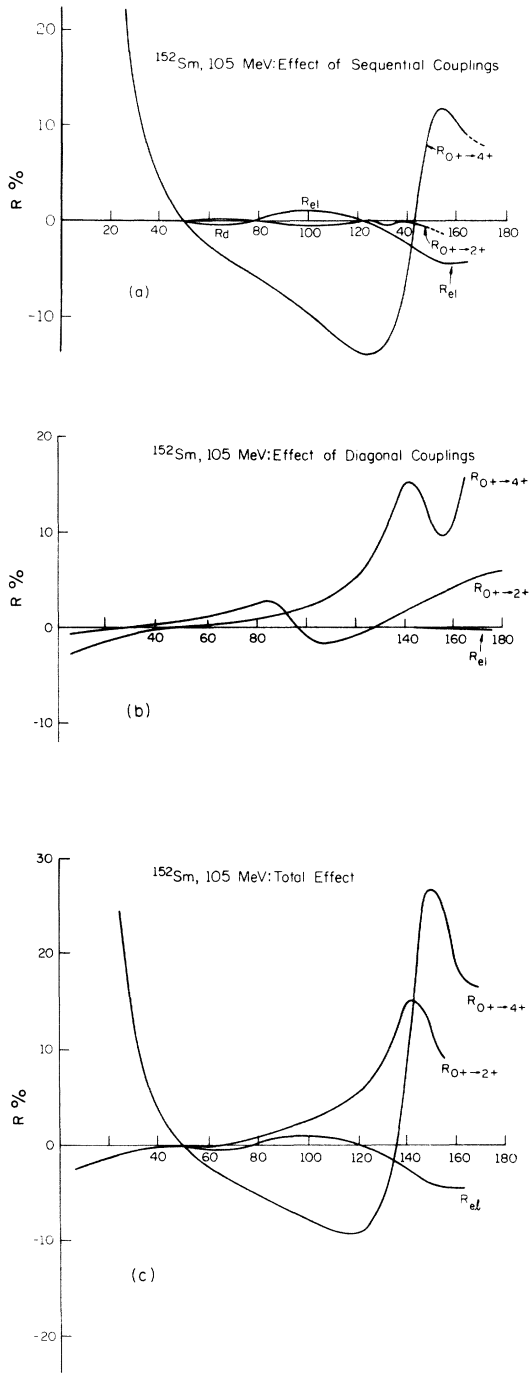

FIG. 4. (a) Angular dependence of R, relative dispersion effects, as defined in Eq. (4) of the text, for the cross sections obtained in mode (a), with only sequential $l=2$ and $l=4$ potentials. (b) $R_{a;b}$, as defined in Eq. (5) of the text. It represents the relative effect of the diagonal $l=2$ and 4 potentials introduced by coupling mode (b), as compared to the effects calculated using mode (a). (c) R, relative dispersion effect as defined by Eq. (4) of the text, for coupling mode (b). This represents all of the coupled-channel effects.

multipole charge densities $\rho_l(r)$. In Fig. (4a), with a linear ordinate, are shown the angular dependences of the relative dispersion effect on the elastic cross section

$$R_{\rm el} = [\sigma_{\rm el} - \sigma_{\rm el}(1 \text{ state})]/\sigma_{\rm el}(1 \text{ state}) \qquad (4a)$$

and of the coupled-channel effects on the inelastic cross sections,

$$R_{i\to f} = [\sigma_{i\to f} - \sigma_{i\to f}(\text{DWBA})]/\sigma_{i\to f}(\text{DWBA}) \ . \qquad (4b)$$

Here, σ(DWBA) is obtained by using the two-state mode (c), shown diagramatically in Fig. 2(c), for the ground state and the particular final state involved. The coupling strength s_l of the transition potential is then reduced to s_l/r, where r is some factor > 1, such as $\sqrt{10}$, and the resulting inelastic cross section is multiplied by r^2. In this manner the coupled-channel effects still present in the two-state calculation are reduced by a factor r^2 relative to the inelastic cross section, which becomes, when these effects are negligible, just the first-order result of the coupling potential, i.e. the distorted-wave Born approximation. As Fig. (4a) reveals, $R_{\rm el}$ is smoothly varying, with an excursion of order 5%, a noticeable correction to the very accurate MIT-NBS data. It is not huge, however, and its inclusion should have only a minor effect on the nuclear parameters previously deduced. The dispersion effect $R_{0+\to 2+}$ on the $0+ \to 2+$ transition is an order of magnitude smaller. Its somewhat irregular behavior may be the result of calculational inaccuracy, although its over-all size is almost certainly no larger than that shown. In the sense of a perturbation expansion in the $l=2$ transition potential, both $R_{0+\to 2+}$ and $R_{\rm el}$ are of second order, so the smallness of $R_{0+\to 2+}$ compared with $R_{\rm el}$ is not an obvious result.

For the $0+ \to 4+$ transition, we check by calculating in mode (c), omitting the 2+ state, that the $l=4$ transition potential is small enough for higher-order effects due to $l=4$ to be negligible. The three-state result of Fig. 4(a) for the $0+ \to 4+$ transition must thus come from the 2+ intermediate state. The effect is big, of order ±15% at large angles, where measurements are usually made. An interesting effect occurs at small angles, where the q^{2l-4} dependence of the DWBA result would predict, for $l=4$, that the cross section should vary like q^4. This behavior is completely modified by the sequential $0+ \to 2+ \to 4+$ excitation, which is mediated by the $l=2$ potentials, and thus varies like q^0, as is evident in Fig. 3. It would be amusing to explore this effect, perhaps by using the $(e, e'\gamma)$ process to identify the inelastic group of electrons.[19]

Differential cross sections obtained with the complete coupling mode (b) at 105 MeV are also represented in Fig. 3, but on that scale only the $0+ \to 4+$ case is visibly different from that obtained with mode (a). The differences are significant on an experimental scale, however, and Fig. 4(b) shows the quantity

$$R_{a:b} = [\sigma_b - \sigma_a]/\sigma_a \qquad (5)$$

for the various transitions. The important contributor to the difference between the modes is the diagonal $l=2$ potential. The effect on $R_{\rm el}$ is seen to be small, as might be expected since the diagonal potential contributes only in third order. On $R_{0+\to 2+}$, however, the correction is of first order in the $l=2$ potential, which explains its very appreciable size.[20] The effect is greatest, however, in $R_{0+\to 4+}$, but only at very large angles.

For completeness, we show in Fig. 4(c) the quantities $R_{\rm el}$, $R_{0+\to 2+}$, and $R_{0+\to 4+}$ obtained with coupling mode (b). These represent the total corrections that must be applied to the single-state or DWBA calculations to allow for coupled-channel effects.

These Zenith calculations were made on both an IBM 360-91 computer and on an IBM 360-75 computer. For the three-state (0+, 2+, 4+) runs, storage of about 360 kilobytes is needed, while for the two-state (0+, 2+) runs, 275 kilobytes suffice. The time taken depends markedly on the accuracy required. To obtain the curves of R shown, it is necessary that differential cross sections are accurate to better than 0.1% at all of the angles quoted. This requires that the partial-wave series for the inelastic amplitudes be continued considerably beyond the F values where nuclear finite size affects the cross sections, and the present limitation on accuracy comes mainly from this source. The particular three-state runs which produced Fig. 3 took 69 minutes on the model-75 computer and 28 minutes on the model-91. One-state runs under comparable conditions take about 10 seconds on the model-75, and about 3 seconds on the model-91. Recent and projected improvements in Zenith will speed up these times significantly, we hope.

V. DISPERSION IN ^{154}Sm

The dispersion effect usually examined theoretically is the contribution to elastic scattering from second-order virtual excitation of another level. Although, as the results reported in Sec. IV show, there are other consequences of channel coupling, for elastic scattering this is the important effect. To explore its behavior economically we use the simplified calculational mode (c) illustrated in Fig. 2(c): The nucleus is assumed to consist of only two states, with $J^p = 0+$, 2+, and the only

Coulomb interaction, besides the monopole potentials, is the $l=2$ transition potential linking the two states. The intrinsic parameters c_0, z_0 of the undeformed Fermi shape are taken to be the same as those of ^{152}Sm.[10] Only a β_2-type deformation is assumed, and when fitted to produce the observed $B_{0+\to 2+}(E2)=4.61\times 10^4\ e^2\,\mathrm{fm}^4$[21] its value is $\beta_2=0.353$. The reason for choosing ^{154}Sm to explore the dispersive effects is now revealed, in that β_2 is 20% bigger than in ^{152}Sm. We shall thus be looking at the biggest elastic dispersive effects to be expected from transitions among the rotational levels in these isotopes. (See, however, Ref. 3.) We are aware, of course, that the restricted parameter choice c_0, z_0, β_2 does produce an appreciable $l=4$ charge density, and that this two-state system would have, in nature, also diagonal $l=2$ and $l=4$ effects in the 2+ state. We omit them so that we may examine the simplest dispersive effects, those associated just with the two states and the transition $l=2$ density. Many approximate calculations of dispersive effects consider only this mode, and thus our results will hopefully provide also a useful benchmark for such calculations.

Figure 5 shows the elastic and inelastic (0+ → 2+) differential cross sections for our model of ^{154}Sm, at $E_0=250$ MeV incident energy. Also shown are the dispersive effects obtained with the two-channel method, specifically

$$D_{\mathrm{el}}=\sigma_{\mathrm{el}}\ (2\ \text{state})-\sigma_{\mathrm{el}}\ (1\ \text{state}) \tag{6a}$$

and

$$D_{0+\to 2+}=\sigma_{0+\to 2+}\ (2\ \text{state})-\sigma_{0+\to 2+}(\mathrm{DWBA})\ , \tag{6b}$$

where the cross section $\sigma_{0+\to 2+}$(DWBA) is actually ten times the two-channel cross section obtained with the coupling strength s_2 reduced to $s_2/\sqrt{10}$. The calculations shown assume zero electron mass and zero excitation energy. (We explore these approximations later.) The quantity D is plotted to show the actual magnitude of changes in the cross sections, without the somewhat spurious structure introduced by calculating the relative effect. We note the complex structure of D_{el}, but the surprisingly smooth form of $D_{0+\to 2+}$. We also note the smallness of the latter quantity.

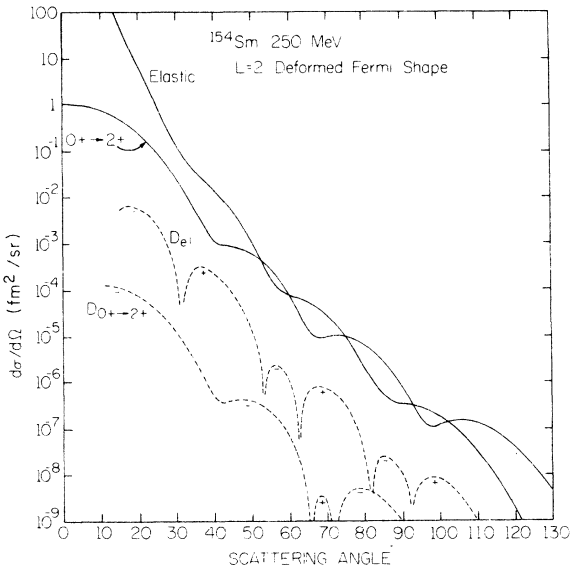

FIG. 5. Differential cross sections at 250 MeV for the $l=2$ deformed model of ^{154}Sm. Also shown are the dispersive differences D defined by Eq. (6).

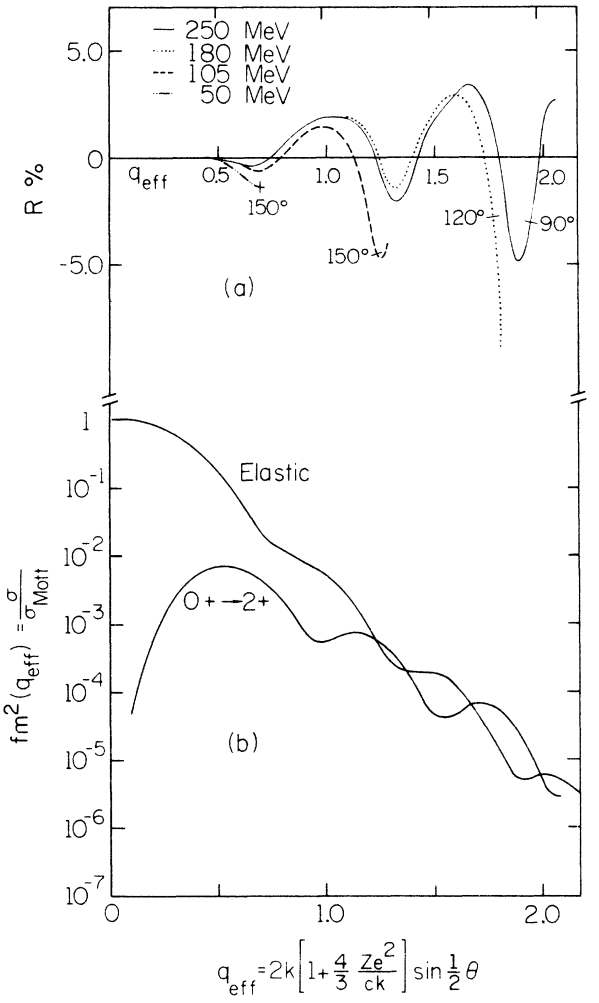

FIG. 6. (a) Relative dispersion effect R_{el}, defined by Eq. (7), for the $l=2$ deformed model of ^{154}Sm at various incident energies, as a function of q_{eff} defined by Eq. (8). (b) $F^2(q_{\mathrm{eff}})$, defined as $\sigma/\sigma_{\mathrm{Mott}}$, for the elastic and $0+\to 2+$ inelastic transitions, as a function of q_{eff}.

This feature has occurred already, in the form of $R_{0+\to 2+}$, in the ^{152}Sm calculations shown in Fig. 4(a). It is because the dispersive effect of sequential coupling on the 0+ → 2+ cross section is so small that we have not made a detailed examination of its q and E dependence in this section.

The relative dispersive effect

$$R_{\rm el} = [\sigma(2 \text{ state}) - \sigma(1 \text{ state})]/\sigma(1 \text{ state}) \qquad (7)$$

is plotted in Fig. 6(a) as a function of

$$q_{\rm eff} = q[1 + \tfrac{4}{3}(Ze^2/c_0)/E_0] \ , \qquad (8)$$

where $q = 2E_0 \sin\frac{1}{2}\theta/\hbar c$. The effective "form factors squared" $F^2 = \sigma/\sigma_{\rm Mott}$ are shown for comparison in Fig. 6(b). The quantity $(\frac{4}{3})(Ze^2/c_0)$ in Eq. (8) is an average of the nuclear attraction, obtained in considering monopole scattering.[22] We observe that in Ref. 10 and other places the length c_0 is replaced by $\langle r^2\rangle^{1/2}$. We know of no theoretical or empirical justification for that substitution. As we see from the figure, however, $R_{\rm el}$, when calculated at various energies which reproduce the same $q_{\rm eff}$, depends markedly on energy in a manner which cannot be removed by any simple redefinition of $q_{\rm eff}$. Up to 50 MeV the dispersive effect is small, reaching a maximum in magnitude of −1.4% at $\theta = 150°$, where $q_{\rm eff} = 0.69$ fm^{-1}. At this $q_{\rm eff}$, but at higher energies, $R_{\rm el}$ tends toward the value −0.4%. The same energy dependence occurs at all higher q, and is clearly not of a kind that can be mimicked by a change in the definition of $q_{\rm eff}$. Thus scattering at a given $q_{\rm eff}$ attained by low E_0 but large θ (say $\theta \gtrsim 120°$) has a significantly different $R_{\rm el}$ from the value obtained with large E_0 and small θ. The connection between this behavior and the large dispersion effects reported in Ref. 2 are commented on at the end of this section.

Since $R_{\rm el}$ is relatively small at energies up to 105 MeV, even for this very deformed nucleus, it is desirable to check whether this result depends on our neglect of, for example, m_e the electron mass and Δ the excitation energy. The approximation $m_e = 0$ we usually employ to reduce computation time, since it halves the number of independent phase shifts. The approximation $\Delta = 0$, as we discuss in Sec. II, may be avoided only if the transition potentials can be made to vanish at the radius $R_{\rm max}$. The stratagem of replacing the transition quadrupole potential by an equivalent monopole excitation, the basis of the claims made in Ref. 2, was examined by us in preliminary calcium calculations.[23] It appears there that the angular structure of the dispersive difference $D_{\rm el}$ is simpler for monopole excitation than for the quadrupole excitation illustrated in Fig. 5. The extra zeros in the quadrupole case mean that on the average the dispersive effects are considerably smaller for quadrupole excitation than for monopole exictation of equivalent strength. We prefer, therefore, to use the alternative trick of applying a "convergence factor" to the $l \neq 0$ potentials. Both the $m_e = 0$ and the $\Delta = 0$ approximations should become better at higher energies, so we explore them here at $E_0 = 50$ MeV, the lowest experimental energy used.[10] Some effects of $m_e \neq 0$ are given numerically in Table I. On cross sections the effect is appreciable theoretically, but even at very backward angles it is hardly noticeable experimentally. On $R_{\rm el}$ there is no detectable effect except at 175°, where

$$R_{\rm el}(m_e) - R_{\rm el}(m_e = 0) \simeq -0.02\% \ .$$

Thus to an accuracy level of 0.1% and energies of 50 MeV and above, it is a completely reliable approximation to neglect the electron mass in calculating $R_{\rm el}$. (For calculating Coulomb contributions to magnetic scattering close to 180° this is not necessarily so, of course.) To check on the effect

TABLE I. Results of Zenith calculations of 50 MeV electrons on the $l = 2$ deformed model for ^{154}Sm. Columns 2 and 3 give the relative effect, on the elastic and 0+ → 2+ inelastic cross sections, respectively, of finite electron mass m_e. Columns 4 and 5 give the elastic dispersive effect $R_{\rm el}$, defined by Eq. (7), for finite m_e and $m_e = 0$, respectively. Columns 6 and 7 show the difference $R_{\rm el}(\Delta) - R_{\rm el}(\Delta = 0)$ for Δ, the nuclear excitation energy, equal to 0.5 and 1.0 MeV. (Experimentally $\Delta = 0.087$ MeV.) *Note that all results are given as percentages.*

	Effect of $m_e \neq 0$				$R_{\rm el}(\Delta) - R_{\rm el}(\Delta = 0)$	
θ (deg)	on $\sigma_{\rm el}$ ×100	on $\sigma_{0+\to 2+}$ ×100	$R_{\rm el}(m_e)$ ×100	$R_{\rm el}(m_e = 0)$ ×100	$\Delta = 0.5$ MeV ×100	$\Delta = 1.0$ MeV ×100
10	0.020	0.014	−0.012	−0.012		
20	0.021	−0.006	0.004	0.004		
30	0.022	0.009	0.025	0.025		
60	0.029	0.013	0.070	0.070	−0.0002	−0.0004
90	0.040	0.023	−0.149	−0.149	0.0004	0.0009
120	0.052	0.041	−0.876	−0.876	0.013	0.027
150	0.078	0.104	−1.384	−1.384	0.049	0.100
175	1.043	1.62	−1.378	−1.358	0.067	0.135

of neglecting Δ, we show also in Table I the difference $R_{el}(\Delta) - R_{el}(\Delta = 0)$, obtained for the artificial values $\Delta = 0.5$ and 1.0 MeV. The actual Δ for ^{154}Sm is 0.087 MeV, and the effect is clearly proportional to Δ. The effect of neglecting Δ in ^{154}Sm thus appears to be negligibly small for this very low-lying state. Our trick of applying the convergence factor to the quadrupole transition potential does affect the inelastic cross section. The convergence factor is arranged to be equal to 1 at $r = \langle r^2 \rangle^{1/2}$, in which region the transition charge density and transition potential are a maximum, but it becomes negligibly small at $r = R_{max}$, where here $R_{max} \simeq 3\langle r^2 \rangle^{1/2}$. As is shown in Fig. 7, the inelastic cross section at very forward angles, which comes from the $l = 2$ excitation potential at very large impact parameters, is considerably reduced by the convergence factor. But over most of the angular range the inelastic cross section is *increased* by about 50%. The finite Δ calculation thus represents the physical situation only approximately. We find it hard to believe, however, that neglecting Δ (the excitation energy) can result in appreciable errors for the present physical situation at energies of the kind considered.

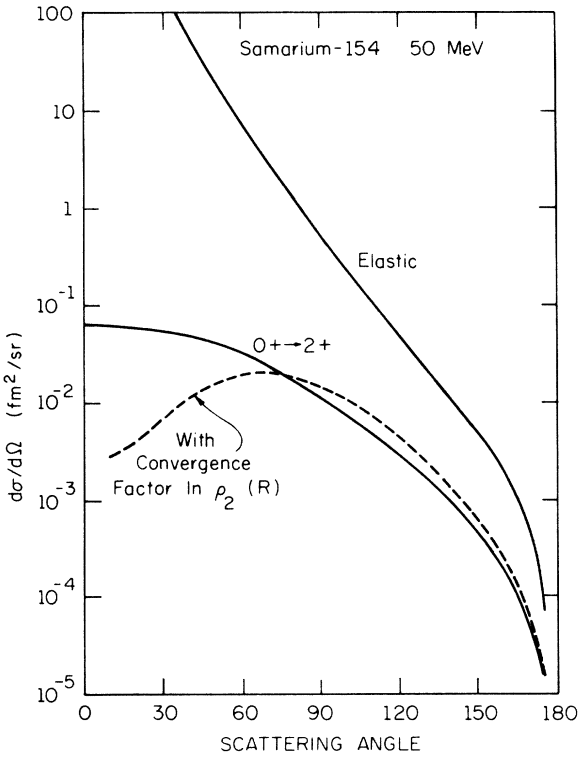

FIG. 7. Differential cross sections for 50 MeV electrons on the $l = 2$ deformed model of ^{154}Sm. The full curves are obtained in the same manner as those shown in Figs. 3 and 5. The dashed curve is the inelastic cross section as it is affected by the convergence factor necessarily applied to the $l = 2$ transition potential when the nuclear excitation energy Δ is taken to be nonzero. It does *not* represent the true effect on the inelastic cross section of neglecting Δ.

In a preliminary account of results on calcium isotopes[23] we reported R_{el} in ^{44}Ca to be of order 2% at 90° and 250 MeV.[24] Our present calculations show R_{el} for ^{154}Sm having an excursion of order 10% under the same conditions. The nucleus ^{44}Ca is not deformed, however, and its $B_{0+\to 2}(E2) = 350$ e^2 fm^4 [21] is very small compared to those of rotational nuclei. We may thus ask how the ^{44}Ca values compare with those of the highly deformed nucleus ^{154}Sm with its much larger $B(E2)$. We do not wish to examine Z-dependent effects in the present work. We examine, however, the effect of another difference between a spherical vibrator and a highly deformed rotator, namely, the radial dependence of the monopole and quadrupole charge densities. The rotational $l = 0$ and $l = 2$ charge densities obtained from the $\rho(\vec{r})$, deformed from $\rho(c_0, z_0; r)$ by the large $\beta_2 = 0.353$, are shown in Fig. 8. As an example of vibrational densities we take the same undeformed Fermi shape, but deform it with only a very small β_2, i.e., $\beta_2 = 0.0035$. The $\rho_0(r)$ is thus effectively the undeformed $\rho(c_0, z_0; r)$ and the $\rho_2(r)$ is proportional to $\partial\rho(c_0, z_0; r)/\partial r$ except near $r = 0$. With these different shapes we use, however, the same *strength* of the quadrupole transition as in the fully deformed case, producing the $\rho_l(r)$ also shown in Fig. 8. The simplified two-channel system employed in this section produces with these $\rho_l(r)$ the cross sections shown in Fig. 9. We observe their close similarity to the cross sections of the fully deformed shape, shown in the same figure, except for a less rapid falloff with angle expected from the smaller surface thickness of the undeformed

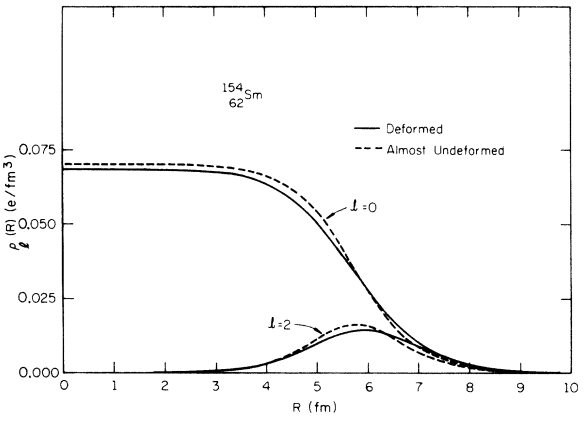

FIG. 8. Multipole charge densities $\rho_l(r)$, defined by Eq. (3), for the $l = 2$ deformed model for ^{154}Sm (full curves) and for the almost undeformed shape (dashed curves).

shape. This results in cross sections which at 90° are larger by about a factor 4. The resulting elastic dispersion, R_{el} is, however, remarkedly close to that of the fully deformed shape, as Fig. 10 reveals. Thus for the rotational nuclear model R_{el} seems to be rather little dependent on the radial shape of $\rho_2(r)$ and $\rho_0(r)$, so long as the transition strength is the same.

We observe another regularity which the present model possesses. For both the almost undeformed and the fully deformed shapes, $\rho_0(r)$ and $\rho_2(r)$ are closely related in that they both come from one deformed shape $\rho(\vec{c}, z_0; \vec{r})$. In vibrational nuclei, it is usually necessary to spoil this close relationship, such as is embodied in the Tassie model, for example, by allowing the transition radius and skin thickness to vary independently of the elastic values. To examine the effect of such a variation, we show also in Fig. 10 the result of increasing the radial scale of $\rho_2(r)$ in the almost undeformed case by 5%. The overall effect is that R_{el} is decreased somewhat. Thus the close relationship contained in the rotational model $\rho_0(r)$ and $\rho_2(r)$, with its concomitant alteration of maxima and minima in the elastic and excitation cross sections, is apparently such as to produce a maximum elastic dispersion effect.

If we compare, finally, the numerical size of R_{el} in ^{154}Sm with that obtained earlier in ^{44}Ca, we have to reconcile an increase in R_{el} by about a factor 5 with an increase in $B(E2)$ by about 130. We observe that $B(El)$, the measure of the strength of a transition of multipolarity l, has dimensions $e^2\,\mathrm{fm}^{2l}$, so that except for $l=0$ its value depends on the size of the system concerned. The transition potential $v_l(r)$ is approximately equal to $s_l R_{nucl}^{-1-l}$ at some nuclear radius R_{nucl} near the edge, and for transitions from the ground 0+ state the strength s_l is related to $B(El)$ by

$$s_l = e[4\pi B(El)/(2l+1)]^{1/2} .$$

Thus the square of the transition potential at R_{nucl}, a measure of the size of the dispersive amplitude, is proportional to $B(El)/R_{nucl}^{2l+2}$. Disregarding the additional 2 in the R_{nucl} exponent as a typical Coulomb manifestation, we surmise that the dispersive effect depends on $B(El)$ according to $B(El)/R_{nucl}^{2l}$. This is equivalent, for a deformed nucleus, to the assumption that the effect depends mainly on the geometric magnitude β of the deformation and is not much dependent on R_{nucl} separately. Assuming an $A^{1/3}$ dependence for R_{nucl} we thus remove a radial scale factor $(154/44)^{4/3} \simeq 5$ from the ratio of $B(E2)$. If we also remove the Z factor $(62/20) \simeq 3$ expressing the fact that what we quote is an interference term with the elastic amplitude, we are left with an expected increase of R_{el} between ^{40}Ca and ^{154}Sm of a factor 9. Thus on the basis of order-of-magnitude arguments R_{el} is about half as big as we expected from our ^{44}Ca calculations. The size thus checks quite well.

The large dispersive effects reported in Ref. 2 were for electrons of order 100 MeV on titanium isotopes. The $B(E2)$ values for the first excited states of ^{46,48}Ti are somewhat larger (by a factor 2 to 5[21]) than that of ^{44}Ca. We deduce from Fig. 6(a) that for ^{154}Sm, dispersive effects at large angles and 105 MeV are *smaller* than those around

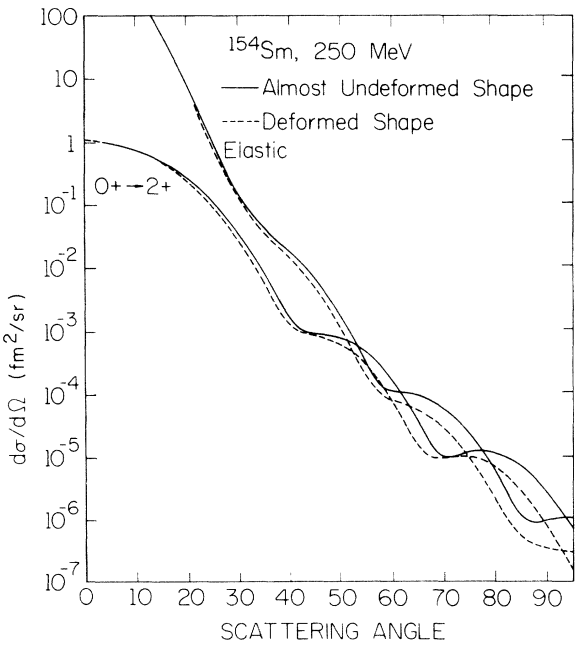

FIG. 9. Differential cross sections for 250 MeV electrons on the almost undeformed model for ^{154}Sm. Also shown (dashed curves) are the cross sections of Fig. 5.

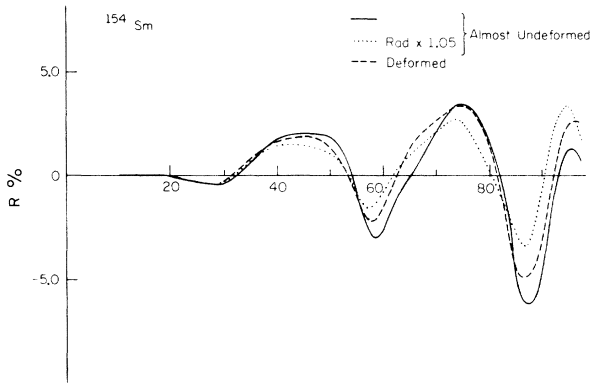

FIG. 10. Relative dispersion effect R_{el} as a function of θ for the $l=2$ deformed model for ^{154}Sm (dashed curve), the almost undeformed shape (full curve), and for the almost undeformed shape with $\rho_2(r)$ increased in radial scale by 5% (dotted).

90° and 250 MeV—the basis of our previous numerical estimates—by about a factor 2. We thus would expect the dispersive effects arising from the low-lying 2+ state alone in ^{46,48}Ti at 100 MeV to be perhaps twice as big as those in ^{44}Ca at 90° and 250 MeV, i.e., about 4%. This number compares to Wall's 10 to 20%.[2] See, however, Ref. 3. The bases for the two values are different in several important respects so no definite conclusion is possible at present. A study of dispersive effects in the Ca and Ti isotopes is in progress.

VI. METHOD FOR DATA ANALYSIS

Given that the dispersive effects calculated in Sec. IV can affect appreciably the analysis of the experimental cross sections, but that the calculation of these effects is as yet time consuming and not automatic, it would seem reasonable to proceed by successive approximations. The quantity $R_{i\to f}$ shown in Fig. 4(c) expresses the fact that the coupled-channel cross section for the nuclear process $1\to f$ is $1+R_{i\to f}$ times as big as the corresponding DWBA (or one-state partial-wave) cross section. It may be hoped from some of the results of Sec. V that R is not too sensitive to the details of the assumed nuclear shape. The assumption that the giant collective states do not contribute sensitively is also required (see Ref. 3). With these assumptions, one may then divide the experimental cross sections by the quantities $1+R_{i\to f}$ and reanalyze the resulting experimental quantities with the customary tools, producing a nuclear shape somewhat different from that of Ref. 10. We may then recalculate the dispersive effects $R_{i\to f}$ with this new shape. Hopefully they will have changed only insignificantly. Otherwise the process can be repeated.

It is unfortunately clear from Fig. 6(a) that $R_{i\to f}$ depends markedly on energy, so that companion figures to Fig. 4(c) at the other experimental energies will be needed. Unless there are compelling reasons for varying E rather than θ, it is certainly simpler theoretically if E is kept fixed in future experiments.

ACKNOWLEDGMENTS

This work was initiated when one of us (R. L. M.) was a graduate student at the University of Illinois. He acknowledges the support of a National Science Foundation Predoctoral Grant during this period. We thank B. C. Clark for consultations and calculations made in the process of checking Zenith. We acknowledge useful physics discussions with P. Axel, L. Cardman, and S. Penner and also very helpful comments on the manuscript from L. Cardman.

---

*Work supported in part by the National Science Foundation under the grant No. GP-25303.

[1]For a summary of work on this topic, see for example H. Uberall, *Electron Scattering from Complex Nuclei* (Academic, New York, 1971), Part B, pp. 757–765.

[2]N. S. Wall, Ann. Phys. (N.Y.) 66, 790 (1971), and other authors cited in this reference.

[3]A complete calculation of dispersive effects would have to include all possible intermediate excited states. Such a calculation is not presently feasible. It is the authors' belief that the giant resonances and quasi-free nucleon states will produce very little nucleus-to-nucleus variation in the dispersive effect. This point requires further study however.

[4]G. Rawitscher, Phys. Rev. 151, 846 (1966).

[5]W. D. Brown and E. Kujawski, Ann. Phys. (N.Y.) 64, 573 (1971); R. Rosenfelder, Nucl. Phys. A216, 477 (1973).

[6]As explained in Sec. III, our treatment of the nuclear excitation energy is not as yet exact.

[7]The eigenchannel theory described in Ref. 1, and exemplified for electron scattering by the calculations of C. Toepffer and W. Greiner [Phys. Rev. 86, 1044 (1969)] makes a quite different attack on the coupled-channel problem. As we understand it, it replaces the direct integration of the coupled wave equations by the diagonalization, in the space of uncoupled single-channel functions, of all of the multipole coupling terms. A detailed comparison of the results of Toepffer and Greiner with those of Zenith on the vibrational nucleus ^{58}Ni will be made soon.

[8]J. M. McKinley, Phys. Rev. 183, 106 (1969).

[9]R. L. Mercer, Ph.D. thesis, Department of Computer Science, University of Illinois, 1972 (unpublished), contains a detailed description of the computational methods and the equations. A summary of the salient points is in preparation by R. L. Mercer.

[10]W. Bertozzi, T. Cooper, N. Ensslin, J. Heisenberg, S. Kowalski, M. Mills, W. Turchinetz, C. Williamson, S. P. Fivozinsky, J. W. Lightbody, Jr., and S. Penner, Phys. Rev. Lett. 28, 1711 (1972).

[11]See D. R. Yennie, D. G. Ravenhall, and R. N. Wilson, Phys. Rev. 95, 500 (1954).

[12]We have also constructed the program Nadir, a more primitive version of the methods described here, which includes only monopole excitation to an arbitrary number of excited states with, however, arbitrary nuclear excitation energies. A one-state version of Nadir which includes a complex monopole optical potential, Cnadir, has been used in calculations of relativistic proton-nucleus scattering [B. C. Clark, A. H. Saperstein, R. L. Mercer, and D. G. Ravenhall, Phys. Rev. C 7, 466 (1973)] and polarization (unpublished). The inclusion of hadronic potentials in Nadir and Zenith will be attempted shortly.

[13]B. C. Clark, as used in, for example, J. Heisenberg,

R. Hofstadter, J. S. McCarthy, I. Sick, M. R. Yearian, B. C. Clark, R. Herman, and D. G. Ravenhall, in *Topics in Modern Physics*, edited by W. E. Brittin and H. Odabasi (Colorado A.U.P., Boulder, Colorado, 1971), pp. 169–189 and in the other work referred to there involving the last three authors named.

[14]B. C. Clark, Ph.D. thesis, Wayne University, 1973 (unpublished).

[15]J. Heisenberg, I. Sick, and J. S. McCarthy, Nucl. Phys. A164, 353 (1971). We thank Professor L. Cardman for running this program.

[16]We thank T. Cooper for communicating to us the complete parameter specification of this analysis.

[17]Other users should note the by now customary barbarism of Eq. (2), with its inconsistently specified $l = 0$ term.

[18]Note that these calculations do not include electric multipole potentials. At the recoil momenta involved, the expected size of electric contributions, $\propto (\Delta E/q)^2$, is very small for $\Delta E = 0.36$ MeV, the largest energy difference involved here.

[19]This is an observation of L. Cardman.

[20]Such a contribution, a reorientation effect, has been included by Toepffer and Greiner, Ref. 7. They also find it to be the dominant contribution to the corresponding inelastic transition.

[21]P. H. Stelson and L. Grodzins, Nucl. Data A1, 21 (1965).

[22]See, for example, R. Yennie, F. L. Boos, and D. G. Ravenhall. Phys. Rev. 137, B882 (1965).

[23]D. G. Ravenhall, in *Proceedings of the International Conference on Photonuclear Reactions and Applications, Asilomar, 1973*, edited by B. L. Berman (Lawrence Livermore Laboratory, Univ. of California, Livermore, 1973), p. 1281.

[24]The value quoted is in fact taken from another calculation (unpublished) which uses the Tassie model with the $B(E2)$ value given in the text.